

**Natural Mexican Clinoptilolite for ethanol dehydration: adsorption-regeneration experimental parameter determination and scaling-up at Pilot Plant****Clinoptilolita natural mexicana para la deshidratación de etanol: adsorción - regeneración y escalamiento de los parámetros experimentales a nivel planta piloto**G. Leo-Avelino¹, G.R. Urrea-García², J. Gómez-Rodríguez¹, S. Perez-Correa¹, M.G. Aguilar-Uscanga^{1*}¹Tecnológico Nacional de México/I. T. de Veracruz, Depto. de Ingeniería Química y Bioquímica/Unidad de Investigación y Desarrollo en Alimentos (UNIDA), Calz. M.A. de Quevedo 2779. Col. Formando Hogar, C.P. 91860, Veracruz, Ver., MÉXICO.²Tecnológico Nacional de México/I. T. de Orizaba, División de Estudios de Posgrado e Investigación, Oriente 9 Emiliano Zapata Sur, C.P. 94320, Orizaba, Ver., MÉXICO.

Received: February 7, 2021; Accepted: DATE

Abstract

The separation of ethanol-water azeotropic mixtures by adsorption-regeneration process using a natural Mexican Clinoptilolite has been studied. For this, the equilibrium parameters were determined from experimental data obtained at the laboratory level, which were used as a starting point for the calculation of a column at Pilot Plant scale. First, on the basis of experimental data from three different sizes of natural Mexican clinoptilolite (1-2, 3 and 5 mm) and two artificial ones with 1 and 3 mm, and from the application of standard fitting techniques: Langmuir, Freundlich and linear model parameters are calculated and compared. Then, the breakthrough curves (BTC) are determined for each zeolite in a packed bed, yielding that the adsorption and capability of natural clinoptilolite is similar to those presented by artificial zeolites. The regeneration method PSA (Pressure Swing Adsorption) was evaluated for each zeolite. Finally, according to the experimental parameters set, a calculation of a pilot-plant scale column is included for a validation and the results are compared with the results obtained at the laboratory scale, which presented a similar behavior. We can conclude that the use of Mexican zeolite in the ethanol dehydration process could be a good low-cost alternative that is easy to apply.

Keywords: Ethanol, dehydration, adsorption, pilot plant, zeolites.

Resumen

En este trabajo se presenta un estudio de la separación de mezclas azeotrópicas de etanol-agua mediante el proceso de adsorción-regeneración utilizando una Clinoptilolita mexicana natural (Zeolita); para ello primero se determinaron los parámetros de equilibrio a partir de datos experimentales obtenidos a nivel laboratorio, de tres tamaños diferentes de clinoptilolita natural mexicana (1-2, 3 y 5 mm) y dos artificiales de 1 y 3 mm, y de la aplicación de técnicas de ajuste estándar: Langmuir, Freundlich y lineal, se calcularon los parámetros de los modelos y se compararon las zeolitas mexicanas contra las comerciales. Luego, se determinaron las curvas de ruptura (CR) para cada zeolita en un lecho empacado, dando como resultado que la capacidad de adsorción de la clinoptilolita natural mexicana era similar a las que presentan las zeolitas artificiales. Así también se evaluó el método de regeneración por oscilación de presión (Pressure Swing Adsorption PSA, por sus siglas en inglés) para cada zeolita y finalmente, de acuerdo con los parámetros experimentales establecidos a nivel laboratorio, se llevo a cabo el cálculo y diseño de una columna a escala planta piloto validándose los resultados obtenidos a escala laboratorio en la columna diseñada y construida. los resultados mostraron un comportamiento muy similar de la curva de adsorción-regeneración tanto en la columna a nivel planta piloto como a nivel laboratorio. Con lo que podemos concluir que el uso de la zeolita mexicana en el proceso de deshidratación de etanol, podría ser una buena alternativa de bajo costo y fácil de aplicar.

Palabras clave: Etanol, deshidratación, adsorción, planta piloto, zeolitas.

*Corresponding author. E-mail: maria.au@veracruz.tecnm.mx
Tel. +52 (229)9345701 ext 211. ORCID ID: 0000-0002-3875-7928.
<https://doi.org/10.24275/rmiq/Proc2358>
ISSN:1665-2738, issn-e: 2395-8472

1 Introduction

In recent years, petroleum reserves have been rapidly depleting with consequent increased cost due to new technological extraction requirements (Agartan *et al.*, 2018; Kuhns and Shaw, 2018). This problem has made anhydrous ethanol an alternative source with wide popularity for providing renewable energy, also presenting energy savings and a substantial reduction in net carbon dioxide emissions into the atmosphere (Singh and Rangaiah, 2017; Kupiec *et al.*, 2014; Ribeiro *et al.*, 2018). Ethanol can be produced industrially by two methods: biomass fermentation and catalytic ethylene hydration (Banat *et al.*, 2000). Ethanol production studies using biomass have been quickly increased due to the availability of a wide diversity of agricultural raw material with fermentable sugars (Partida-Sedas *et al.*, 2016; Corro-Herrera *et al.*, 2018; Delfín-Ruíz *et al.*, 2020; Morales-Martínez *et al.*, 2020).

To obtain anhydrous ethanol, many problems must be addressed, one of them being the energy consumed in the separation and purifying process, distillation is infeasible since at atmospheric pressure ethanol forms an azeotrope with water at a temperature of 78.15 °C (Jeong *et al.*, 2012). Alternative recovery methods have been developed to break the azeotrope, such as azeotropic, extractive, vacuum and reactive distillation, pervaporation and adsorption by molecular sieves (Al-Asheh *et al.*, 2015). Although “pervaporation is a new generation of membrane separation technology”, its limitation lies in scaling-up due to high cost in terms of membrane fabrication (Abdeen *et al.*, 2011; Kaminski *et al.*, 2008).

Ethanol dehydration by adsorption is a common high performance method requiring low energy input and is often “capable of producing very pure product” (Abdeen, *et al.*, 2011). The purpose of this study is to find low cost adsorbent material with an effective adsorption capacity that which reduces investment costs. The major and most abundant microporous sorbents in nature are zeolites, with hydrophilic properties suitable for water-ethanol separation. Natural zeolites are crystalline, hydrated aluminosilicate minerals known as “molecular sieves” with a framework structure-enclosing cavity occupied by large ions and water molecules. Adsorption behavior depends on several parameters, such as porous structure, the Si/Al ratio of the zeolite framework and the species of the exchanged cation (Smith 1984). To produce anhydrous ethanol, water is removed by with 3Å pore size zeolite as 2.8 Å molecule size water is adsorbed, while 4 Å ethanol molecules are not. There are many natural zeolites identified in the world, such as clinoptilolite, mordenite, phillipsite, chabazite, stilbite, analcime and laumontite, among others. Clinoptilolite is the most abundant natural zeolite in the world (Wang and Peng, 2010). In Table 1, the chemical composition of natural clinoptilolite from different countries is presented. The performance of zeolites as adsorbents for ethanol dehydration is evaluated by measuring adsorption isotherms and breakthrough curves. Adsorption isotherms are plots describing the phenomenon governing the retention or release of a substance from the aqueous porous media to a solid at constant temperature condition. There are many equilibrium isotherm models presented in literature, formulated in terms of three fundamental approaches: kinetic considerations, thermodynamics and potential theory (Foo and Hameed, 2010).

Table 1. Chemical composition of natural zeolites in the world.

Zeolite	Chemical composition (%)							
	SiO ₂	Al ₂ O ₃	Fe ₂ O ₃	CaO	MgO	Na ₂ O	K ₂ O	TiO ₂
Turkish clinoptilolite	70	12.4	1.21	2.54	0.83	0.28	4.46	0.089
Iranian clinoptilolite	70	10.46	0.46	0.2	-	2.86	4.92	0.02
Cuban clinoptilolite	62.35	13.14	1.63	2.72	1.22	3.99	1.2	-
Chinese clinoptilolite	65.52	9.8	1.04	3.17	0.61	2.31	0.88	0.21
Croatian clinoptilolite	64.93	13.39	2.07	2	1.08	2.4	1.3	-
Ukrainian clinoptilolite	66.7	12.3	1.05	2.1	1.07	2.06	2.96	-
Australian clinoptilolite	68.26	12.99	1.37	2.09	0.83	0.64	4.11	0.23
Mexican clinoptilolite*	68.2	12.7	2.2	0.48	0.58	3.1	2.9	-

^aFrom Wang *et al.*, 2010

*Used in this experimental study

Yamamoto *et al.*, (2012) evaluated the adsorption isotherms of five different zeolites types and they determined that the Langmuir model could describe the equilibrium adsorption of water on zeolites in ethanol more accurately than the Freundlich model. Karimi *et al.*, (2016) evaluated the natural clinoptilolite from east Semnan, Iran, and the results regarding adsorption isotherms agree with Yamamoto *et al.*, (2012). Ivanova *et al.*, (2009) evaluated natural clinoptilolite from Rhodope Mountain in Bulgaria and they inferred that it shows a strongly favorable equilibrium and high separation efficiency to water. Ivanova and Karsheva (2010) evaluated the same natural clinoptilolite but treated with acid solutions to dissolve some amorphous impurities blocking the pores, with results proving that there was no change in adsorption capacity.

The characteristics of zeolite packed beds for anhydrous ethanol production are revealed by measuring the BTC, that provides parameters such as adsorption capacity, breakthrough time and purity obtained. Tihmillioglu and Ulku (1996) evaluated the performance in a packed bed of natural clinoptilolite from Bigadic, Turkey and they determined the adsorption capacity of $0.13 \text{ kg}_{\text{water}}/\text{kg}_{\text{zeolite}}$; in comparison the natural clinoptilolite from Qazvin, Iran has $0.027 \text{ kg}_{\text{water}}/\text{kg}_{\text{zeolite}}$ adsorption capacity at 1 bar and 14 mL/min flow rate (Karimi *et al.*, 2016).

The adsorption capacity during the dehydration process decreases in a certain time, the quality of the product changes due to this, the zeolite has been saturated with the adsorbed liquid, the liquid must be released to return the original adsorption capacity to the zeolite, this allows its reuse in the adsorption process (adsorption - desorption cycle). To counteract the deterioration of zeolites, different regeneration methods have been developed such as Pressure swing adsorption (PSA).

In the PSA process, desorption is carried out by reducing the pressure until a constant temperature is maintained, subsequently a low-pressure packed bed purge is performed, for which an inert agent is used. Kupiec *et al.*, (2014), consider a sequential process

of pressure swing adsorption, consisting of two steps: an ambient pressure adsorption and a low pressure purging. Jeong *et al.*, (2012) studied a PSA method to ethanol dehydration in a Pilot Plant scale, consisting in four step-loop: adsorption, depressurization, purge, pressurization (Rumbo-Morales *et al.*, 2018). The zeolites regeneration is a multilevel process due to bi-porous structure and bifurcation structure of crystallite, according to that, the gradual water release is observed by Gabruś *et al.*, (2015). The aim of the present work is to determine the characteristics of water adsorption and desorption during ethanol dehydration, on natural Mexican clinoptilolite with three different particle sizes and compare them with two different types of artificial zeolites. The performance of zeolites as adsorbent material for ethanol dehydration is evaluated by the adsorption isotherm and the BTC of the packed bed. The regeneration of each zeolite by PSA method is evaluated for re-use in adsorption process. A pilot plant scale packed bed column array is designed based on parameters obtained of the natural Mexican clinoptilolite particle size selected with the highest performance.

2 Materials and methods

2.1 Adsorption isotherms

Natural Mexican zeolite, clinoptilolite, was supplied by Procomine S RL of CV with three particle sizes, zeolite #1 (1-2 mm), zeolite #2 (3 mm) and zeolite #3 (5 mm), there were examined and their performance in the adsorption of water in ethanol mixture were compared with two artificial zeolites: LV-NENG (1 mm) and Sorbead (3 mm). The properties of the zeolites are summarized in Table 2.

Zeolite samples were preconditioned by thermal activation in a furnace (thermo scientific Lab line) at 200 °C for 24 hours and then stored in a laboratory vacuum desiccator before use them in equilibrium studies.

Table 2. Physical-chemical properties of evaluated zeolites.

Zeolite	SiO ₂ wt. %	Al ₂ O ₃ wt. %	CaO wt. %	Fe ₂ O ₃ wt. %	MgO wt. %	Na ₂ O wt. %	K ₂ O wt. %	Porosity %	Pore diameter Å	Form	Particle size, mm
Clinoptilolite	68.2	12.7	0.48	2.2	0.58	3.1	2.9	45 -50	3	amorphous	1, 3, 5
LV-NENG	2	1	-	-	-	0.33	0.66	20 - 80	3	spheric	1
Sorbead	12	12	-	-	-	0.48	0.72	30 -65	3	spheric	2.6

For adsorption isotherm measurements, 5 g of each zeolite were added to 50 mL ethanol - water mixture in the range of 3.5 - 8 wt.%. The mixture was sealed in a hermetic glass, shaken at 180 rpm, at ambient temperature (25 °C) for 24h. The linear, Langmuir and Freundlich isotherm models were used for description of the adsorption process (Eqs. 1, 2 and 3 respectively).

$$q_e = kc_e \quad (1)$$

$$q_e = \frac{q_0 K_L c_e}{1 + K_L c_e} \quad (2)$$

$$q_e = K_F c_e^{1/n} \quad (3)$$

where q_0 and c_e are the amount of solute adsorbed per unit solid weight and the remaining water concentration in ethanol at equilibrium, respectively; K_L is the Langmuir constant, n is a dimensionless constant which indicates the heterogeneity of the adsorption sites and K_F is the Freundlich constant.

2.2 Measurement of packed bed BTC

A laboratory scale fixed bed adsorption column has been designed as is shown schematically in Figure 1.

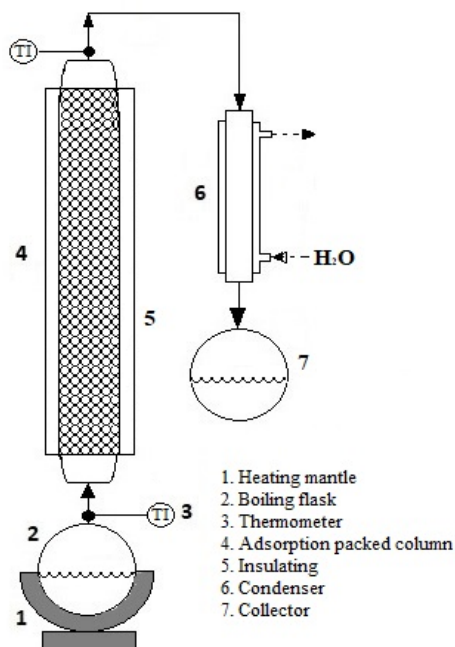


Fig. 1. Schematic diagram of laboratory scale fixed bed adsorption column.

The dimension of the column are diameter of 2.5 cm and length of 60 cm, the wall of the column was insulated to avoid heat loss. The vapor was boiled up from a 1000 mL flask heated by an electric mantle; the concentration of ethanol introduced in the flask was $1.97 \times 10^3 \text{ molm}^{-3}$ at a constant flow rate of $8 \text{ cm}^3\text{min}^{-1}$. The operation pressure was assumed constant at 1 atm. The exit stream of the column was condensed and the temperature of the jacket in the condenser was controlled and kept constant by a recirculating water bath. The column was filled with 200 g of each zeolite described previously to evaluate the breakthrough curve. Liquid output samples were collected every 3 minutes, and the water content of the samples was measured using a Karl Fischer titrator. The breakthrough curve was drawn as the relationship between time and water concentration in the output mixture. According to Eq. 4, total adsorption capacity would be calculated.

$$Q = \frac{F \rho_f c_0}{w} \int_0^{t_R} \left(1 - \frac{c_t}{c_0}\right) dt \quad (4)$$

where, F , ρ_f , c_0 , c_t , w and t_R are flow rate of the ethanol-water mixture, mixture density, water feed concentration, water output concentration, zeolite weight in the packed bed and breakthrough time, respectively. The breakthrough time was considered when c_t/c_0 ratio is 0.05.

2.3 Regeneration by PSA method

The regeneration process was carried out in situ after saturation, using Pressure swing adsorption (PSA) process. In the PSA process the packed bed was subjected to a vacuum by mean of a 1/2 hp vacuum pump, anhydrous ethanol vaporized flowing from the bottom to the top of the column, the condensed vapors will be taken as sample every 2 minutes. The water content will be determined with the Karl Fischer equipment presenting the results in a desorption curve.

2.4 Scaling up to a Pilot Plant

The laboratory scale test column was used for pilot plant scale design of a packed bed column; consider a designed capacity of anhydrous ethanol production of 150 L/day and the procedure for the design was as follows:

- i. Filtration rate of the laboratory scale test was calculated thus:

$$FR = \frac{F}{A} \quad (5)$$

where FR is the filtration rate, F and A are flow rate and cross sectional area respectively.

- ii. Cross sectional area of the packed column was calculated by the following equation:

$$A = \frac{F_2}{FR} \quad (6)$$

where F_2 is the flow rate at pilot plant scale, with this parameter column diameter could be obtained.

- iii. Fraction of capacity left unused, LUB , in a laboratory scale column was calculate as follow

$$LUB = L \left(1 - \frac{t_b}{t^*} \right) \quad (7)$$

where L is the length of the column, t_b and t^* are breakthrough time and initial time, respectively.

- iv. Zeolite mass required in the pilot plant scale packed column was obtained by

$$V_{PB} = \pi * r^2 * h \quad (8)$$

To avoid pressure drops in the packed bed column, it is important to consider in the design a height /diameter ratio of at least 1:20 (Teo and Ruthven, 1986). To scaling up the adsorption process was taken into account two columns for a continuous dehydration.

3 Results and discussion

3.1 Characterization of Mexican zeolite

A micrograph of the natural Mexican clinoptilolite, artificial zeolites LV-NENG and Sorbead used in this work are presented in Figure 2 at 5kx and 20kx magnification, obtained from a scanning electron microscope (SEM), showing the inside morphologic porosity and crystallinity surface of the material. The presence of crystallinity, surface roughness and impurities are characteristic aspects of the heterogeneity of the porous media of the material.

Natural zeolites, in contrast to synthetic zeolites, are mainly made up of two types of porosity: Primary (attributed to the presence of micropores) and secondary (due to mesopores). The secondary porosity that normally conforms to natural zeolites allows phenomena such as the adsorption of relatively large molecules to take place in them, which play a very important role in very specific processes such as diffusion and heterogeneous catalysis. (Horike *et al.*, 2009).

These types of aspects are the reason for the existence of pores of different shapes and sizes that have a phenomenological influence on the filling process of the pores and are regularly reflected by changes in the slope of the adsorption curves, with notable deviations (positive or negative). Characterization studies allow us to distinguish between this pore filling processes with respect to adsorption processes that develop on surfaces of different topologies of natural or artificial zeolites.

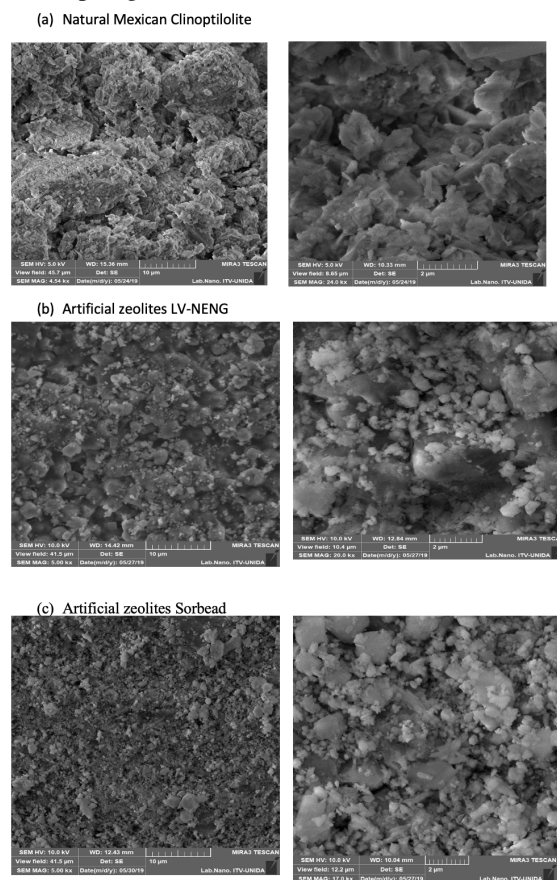


Fig. 2. SEM image of Mexican Clinoptilolite Zeolite (a), LV-NENG (b) and Sorbead (c).

Table 3. Parameters of Freundlich, Langmuir and linear models.

Zeolite	Freundlich model			Langmuir model			linear model	
	K_F	n	R^2	q_0	K_L	R^2	K	R^2
#1	0.518	1.044	0.9996	0.5202	2019.56	0.9926	0.001	0.985
#2	1.5107	3.3176	0.9825	5.211	1386.2	0.9843	0.001	0.9641
#3	0.148	0.0975	0.9585	0.3598	3521.28	0.9646	3×10^{-5}	0.9763
LV-NENG	0.2882	0.058	0.962	0.3041	1353.44	0.9833	1×10^{-5}	0.9443
Sorbead	0.1501	0.173	0.9783	0.2886	1053.11	0.9725	8×10^{-5}	0.9377

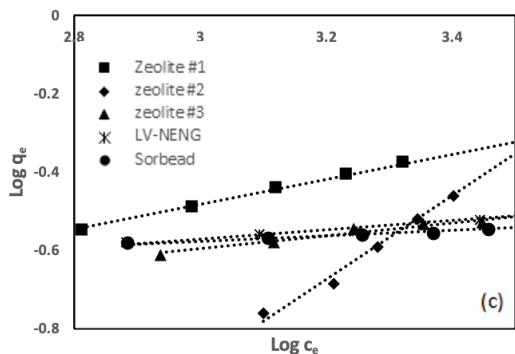
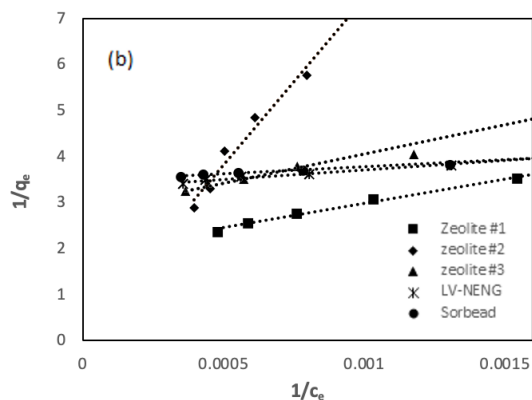
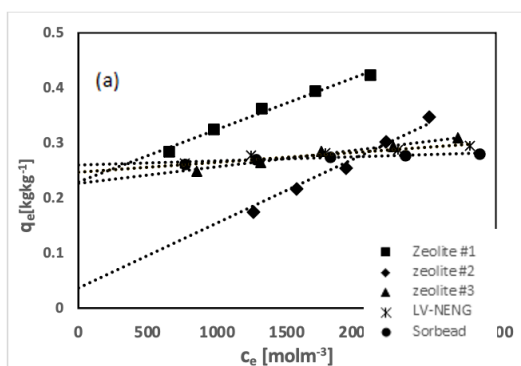


Fig. 3. Adsorption isotherms of water - ethanol mixture on zeolites at 25 °C. (a) Linear model, (b) Langmuir model and (c) Freundlich model.

3.2 Isothermal adsorption curves

To evaluate the performance of this natural zeolite in the ethanol dehydration process, the isotherm adsorption (q_e) of water in ethanol for each zeolite was determined. Eq. 1 representing the equilibrium relationship between water concentration and the quantity of water adsorbed on zeolites [$kg_{water}/kg_{zeolite}$], which was applied to the results of the tests. The determination of the constants (c_e vs. q_e) of the Langmuir model ($1/c_e$ vs. $1/q_e$) and the Freundlich model ($\log c_e$ vs. $\log q_e$) was carried out by fitting the linear models to the (Equations 1, 2 and 3, respectively). Graphs are presented in Figure 3, representing adsorption isotherms for zeolites #1, #2, #3, LV-NENG and Sorbead, supporting a highly favorable adsorption. The R^2 value was determined to compare the precision of the adjustment of the three models. According to results presented in Table 3, the linear model presents a k value close to zero, which represent low adsorptivity, this is not a characteristic of the zeolites, the Langmuir model describes more accurately the equilibrium of adsorption of water than Freundlich model, indicating that this process would be expressed as a monolayer adsorption model and all porous sites could be considered as identical. Similar behavior was observed by Tihmillioglu and Ulku (1996).

The parameter q_0 determined for each zeolite indicates the maximum capacity adsorption of the zeolite expressed as $kg_{water}/kg_{zeolite}$; in this case it was found that natural zeolite #1 has a higher adsorption capacity followed by zeolite LV-NENG, due to their small particle size (1 - 2 and 1 mm, respectively). This behavior is attributed to the fact that more surface area is found in a determined volume and thus a major contact surface, a conclusion that agree with Teo and Ruthven (1986), for artificial 3 Å zeolites. Different outcomes showed by Karimi *et al.*, (2019) indicated that the particle size has an important role in final ethanol concentration and uptake, large particle size

will reduce final uptake due to the lower specific surface area. Yamamoto *et al.*, (2012) investigated on different zeolite particle size and revealed that the uptake values for particle sizes (75 - 100 μm) were at least 10% higher than that of particle sizes (150 - 250 μm). Thus, the particle size of adsorbents has a significant effect on the final solute concentration, and hence on the overall performance of the adsorption process.

For the adsorption of water, the natural clinoptilolite presents a favorable equilibrium in the liquid phase, showing a high selectivity to water in contrast to ethanol. The selected model would be used in the future to carry out simulations of the process or in the design of scaling-up to an industrial plant.

3.3 Breakthrough curves

The breakthrough curves were determined in a packed bed for the five zeolites previously evaluated, using a $1.3 \times 10^{-7} \text{ m}^3/\text{s}$ flow rate with 3.5 wt% concentration of water in ethanol. The results are shown in Figure 4: graph (a) represents the experimental studies of natural clinoptilolite zeolites with three different particle sizes and (b) the comparison of performance of the best natural zeolite behavior (#2) and two artificial zeolites. The breakthrough times t_b , when $c_t(c_0 = 0.5)$, and the quantities of water adsorbed (Q) are summarized in Table 4. The artificial zeolite LV-NENG presents a high breakthrough time (900 seconds) followed by natural zeolite #2 with 720 seconds. During the test performed with natural zeolite #1 pressure drop was

present, potentially attributable to the form and size of the particle. According to results, natural clinoptilolite #2 with 3 mm particle size is competitive in the adsorption process compared with artificial zeolites, which have a market value 99.8% higher than natural zeolites.

3.4 Regeneration process

The breakthrough curve of desorption is presented in Figure 5, for the PSA regeneration for each zeolites. A low regeneration time presented in Zeolites #1 y #3, this behavior was expected due to a low adsorption time. The natural zeolite #2 presented a regeneration time of 12 minutes, equal to adsorption time, which is an ideal behavior to avoid offset in the alternately adsorption-regeneration process. The regeneration time for LV-NENG and Sorbead zeolites was equal to breakthrough time in adsorption process. In addition to the efficient regeneration of saturated packed bed, a concentrated alcohol solution was recovered, which could be reprocessed.

Table 4. Quantity of water adsorbed (Q) and breakthrough time (t_b) of zeolites.

Zeolite	Q [kgkg^{-1}]	t_b [sec]
#1	0.094	540
#2	0.125	720
#3	0.013	180
LV-NENG	0.186	720
Sorbead	0.106	540

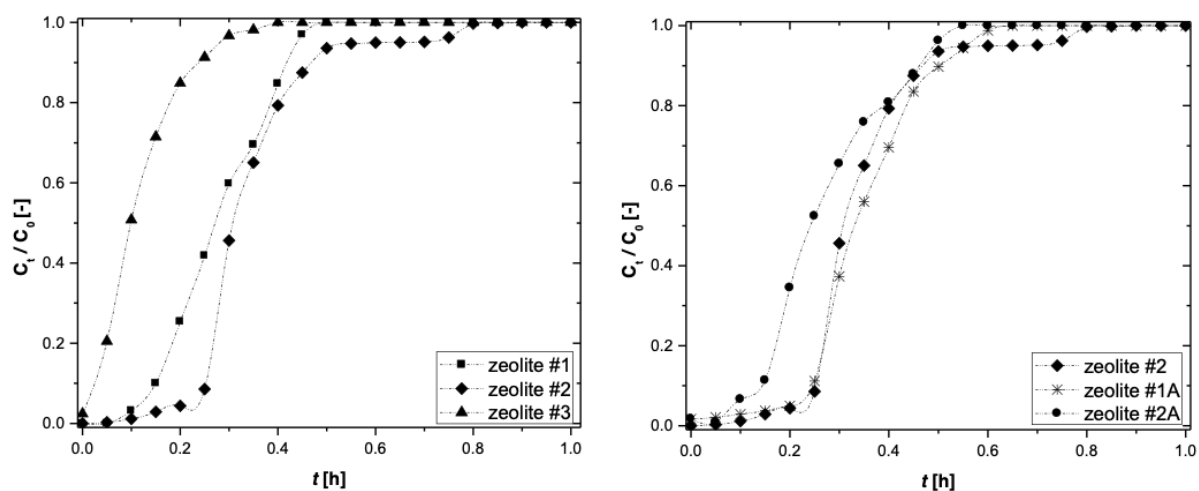


Fig. 4. Breakthrough curve of each zeolite evaluated.

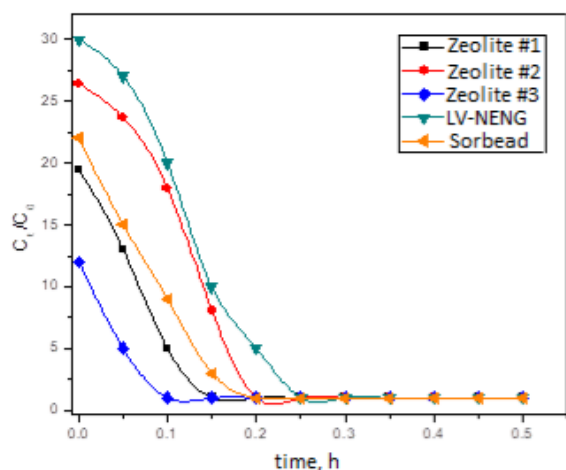


Fig. 5. Regeneration of zeolites using PSA method.

3.5 Pilot plant scale-up and validations

The laboratory scale column parameters previously obtained were used for the pilot plant scale-up design of a packed bed column. The calculation of the design is presented below:

- i. Filtration rate of the laboratory scale column
The diameter of the column at laboratory scale was 2.5 cm and the value of F was $8 \text{ cm}^3/\text{min}$, therefore the area value was $A = 4.9 \text{ cm}^2$, then the filtration rate was

$$FR = 1.63 \text{ cm/min} \quad (9)$$

- ii. Calculation of area of the packed bed column in a pilot plant scale

Considering F_2 as $150 \text{ cm}^3/\text{min}$, which is obtained for the second distillation column

$$A = 92.02 \text{ cm}^2 \quad (10)$$

Thus, the diameter of the column $d = 10.8 \text{ cm}$ and according to the relationship height - diameter of at least 1:20, a proposed height is 2.4 meters.

- iii. Fraction of capacity left unused (laboratory scale column)

$$LUB = 27.5 \text{ cm} \quad (11)$$

The unused percentage of the packed bed is 55%.

- iv. Zeolite mass required in the scaled - up packed column, considering the density of natural zeolite #2 1.16 g/cm^3

$$M = 17 \text{ kg natural zeolite} \quad (12)$$

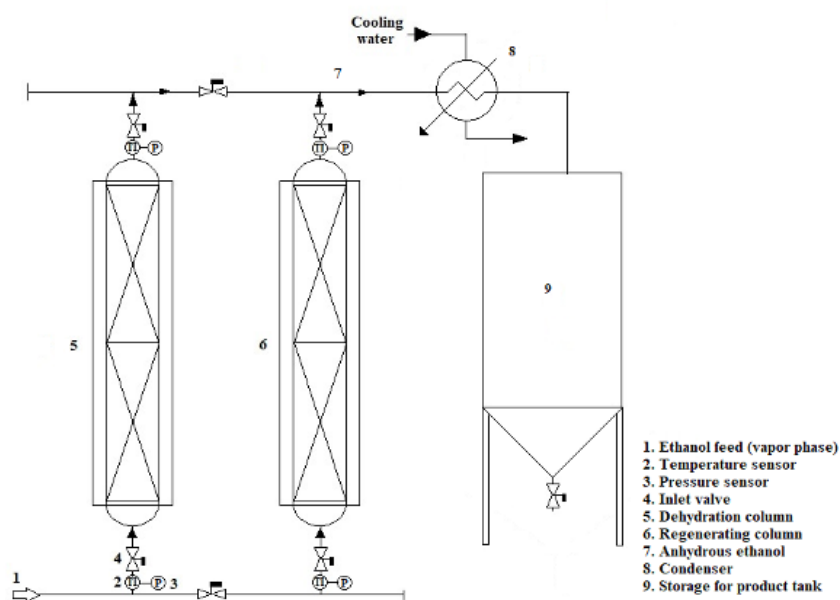


Fig. 6. Process of dehydration/regeneration for the pilot plant design.

The dimensions obtained in the calculation for the design of the adsorption columns ensure the desired concentration without presenting high pressure drops in the system as well as optimal energy consumption. The system has two packed columns (Figure 6), one for the adsorption process for a period of 12 minutes until saturation and the other for regenerating the packed bed and vice versa, with a production capacity of anhydrous ethanol of 9 L/h. This arrangement is recommended even at industrial scale.

The columns designed previously were constructed and installed in the pilot plant, with the purpose of perform the results validation obtained at laboratory scale previously presented. The columns were filled with the natural zeolites #2 selected as best performance in this study. The breakthrough curve analysis was evaluated in the columns to validate the scaling up. The results were compared with the breakthrough curve obtained for natural zeolite #2 study evaluated in laboratory scale, this comparison is presented in Figure 7, according to breakthrough curves the performance of both processes show a similar behavior. The breakthrough time presented for laboratory scale was 12 min and for pilot plant was 13 min, this will be attributed to the characteristics of the packed bed filled in.

Cost studies simulation made up by Hanchate, *et al.*, (2019) of the separation-dehydration processes at pilot scale, operating cost comprises of the cost for molecular sieves 3A and cost of energy consumed in the reboiler and condenser of the distillation tower, pumping of feed and reflux to distillation column, cost of vapor super heater, dehydration column condenser and compressor, an estimated total annualized cost for ethanol recovery process was \$186.58 dls/ton.

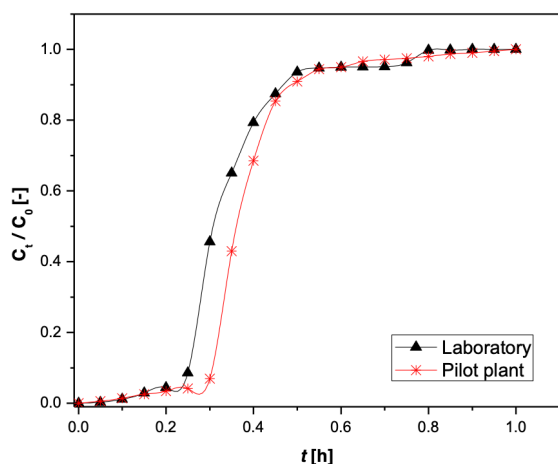


Fig. 7. Breakthrough curve comparison for natural Zeolite #2 on laboratory and pilot plant scale.

Conclusions

In this research work, the adsorption characteristics of different particle size of Mexican natural clinoptilolite were investigated to evaluate the performance in dehydration ethanol process. The Langmuir model was more accurate for describing the adsorption of water on zeolite than the Linear and Freundlich models. The breakthrough curve results of water on molecular sieves showed that zeolite #2 exhibits a competitive result in terms of breakthrough time and adsorption - regeneration capacity compared with artificial material. Results showed that using an optimum size, bioethanol final concentration could reach more than 99.5%v/v. The obtained parameters from laboratory scale were used to design and build a packed bed column scale-up using two columns for an adsorption - desorption cyclic process, the validation was performed comparing the results of breakthrough curve at laboratory studies presenting a similar behavior, the capacity of process at pilot plant scale was 9 L/h of anhydrous ethanol. The implementation of this process to full scale using the Mexican natural zeolite clinoptilolite can significantly reduce investment costs.

Acknowledgements

The authors acknowledge the financial support provided by CONACyT-SAGARPA (Project 173411) and the critical reading by Patricia Margaret Hayward-Jones, MSc and Dulce María Barradas-Dermitz, MSc.

Nomenclature

α	surface area of a particle per unit volume of a packed bed [m^2/m^3]
c	bulk water concentration [mol/m^3]
c_e	water equilibrium concentration of water [mol/m^3]
c_0	water initial concentration [mol/m^3]
c_t	water exit concentration [mol/m^3]
F	volume flow rate [m^3/s]
K_F	Freundlich constant [$\text{kg}/\text{kg}(\text{mol}/\text{m}^3)^{1/n}$]
K_L	Langmuir constant [m^3/mol]
m	mass of zeolite used for equilibrium adsorption measurement [kg]

n	Freundlich constant
Q	amount of adsorbed water in ethanol [kg water/kg zeolite]
q_e	equilibrium adsorbed amount of water in ethanol [kg water/kg zeolite]
R^2	mean squared error
t	time [s]
t^*	initial time
tb	breakthrough time [s]
V	volume of mixture ethanol - water [m ³]
w	adsorbent mass in packed bed [kg]

References

- Abdeen, F.R.H., Mel, M., Al-Khatib, M. and Azmi, A.S. (2011) Dehydration of ethanol on zeolite based media using adsorption process. *Proc CUTSE Int Conf* 3, 312-322.
- Agartan, E., Gaddipati, M., Yip, Y., Savage, B. and Ozgen, C. (2018). CO₂ storage in depleted oil and gas fields in the Gulf of Mexico. *International Journal Greenhouse Gas Control* 72, 38-48. <https://doi.org/10.1016/j.ijggc.2018.02.022>.
- Al-Asheh, S., Banat F. and Al-Lagtah, N. (2004). Separation of ethanol-water mixtures using molecular sieves and biobased adsorbents. *Chemical Engineering Research and Design* 82, 855 - 864. <https://doi.org/10.1205/0263876041596779>
- Banat, F., Abu Al-Rub, F. and Simandl, J. (2000) Analysis of vapor-liquid equilibrium of ethanol - water system via headspace gas chromatography: effect of molecular sieves. *Separation and purification Technology* 18, 111-118. [https://doi.org/10.1016/S1383-5866\(99\)00057-X](https://doi.org/10.1016/S1383-5866(99)00057-X)
- Bourriot, S., Garnier, C. and Doublier, J.L. (1999). Phase separation, rheology and microstructure of micellar casein-guar gum mixtures. *Food Hydrocolloids* 7, 90-95. [https://doi.org/10.1016/S0268-005X\(98\)00068-X](https://doi.org/10.1016/S0268-005X(98)00068-X).
- Corro-Herrera, V.A., Gómez-Rodríguez, J., Hayward-Jones, P.M., Barradas-Dermitz, D.M., Gschaedler-Mathis, A.C. and Aguilar-Uscanga, M.G. (2018) Real-time monitoring of ethanol production during *Pichia stipitis* NRRL Y-7124 alcoholic fermentation using transfection near infrared spectroscopy. *Engineering in life sciences* 18, 643-653. <https://doi.org/10.1002/elsc.201700189>
- Delfín-Ruíz, M.E., Calderón-Santoyo, M., Ragazzo-Sánchez, J.A., Gómez-Rodríguez, J., López-Zamora, L. and Aguilar-Uscanga, M.G. (2020) Ethanol production from enzymatic hydrolysates optimized of *Agave tequilana* Weber var. azul and *Agave karwinskii* bagasses. *Bioenergy research*. <https://doi.org/10.1007/s12155-020-10196-7>.
- Foo, K. and Hameed, B. (2010) Insights into the modeling of adsorption isotherm systems. *Chemical Engineering Journal* 156, 2-10. <http://dx.doi.org/10.1016/j.cej.2009.09.013>
- Gabruś, E., Nastaj, J., Tabero, P. and Aleksandrak, T. (2015) Experimental studies on 3Å and 4Å zeolite molecular sieves regeneration in TSA process: Aliphatic alcohols dewatering-water desorption. *Chemical Engineering Journal* 259, 232-242. <https://doi.org/10.1016/j.cej.2014.07.108>
- Hanchate, N., Kulshreshtha, P., Mathpati, C.S. (2019). Optimization, scale-up and cost estimation of dehydration of ethanol using temperature swing adsorption. *J. Env. Chem. Eng.* 7, 102938. <https://doi.org/10.1016/j.jece.2019.102938>
- Horike, S., Shimomura, S., Kitagawa, S., (2009). Soft porous crystals. *Nat. Chem.* 1, 695 - 704. <http://doi.org/10.1038/nchem.444>
- Ivanova, E., Damgaliev, D. and Kostova, M. (2009) Adsorption separation of ethanol - water liquid mixtures by natural clinoptilolite. *Journal of the University of Chemical Technology and Metallurgy* 44, (3) 267 - 274.
- Ivanova, E., Karsheva, M. (2010). Ethanol vapors adsorption on natural clinoptilolite - equilibrium experiments and modelling. *Separation Purification Technology* 73, 429-431. <http://dx.doi.org/10.1016/j.seppur.2010.04.022>.
- Jeong, J., Jeon, H., Ko, K., Chung, B. and Choi, G. (2012) Production of anhydrous ethanol

- using various PSA (Pressure Swing Adsorption) processes in pilot plant. *Renewable Energy* 42, 41 - 45. <https://doi.org/10.1016/j.renene.2011.09.027>
- Kaminski, W., Marszalek, J. and Ciolkowska, A. (2008) Renewable energy source - Dehydrated ethanol. *Chemical Engineering Journal* 135, 95-102. <http://dx.doi.org/10.1016/j.cej.2007.03.017>
- Karimi, S., Ghobadian, B., Omidkhan, M., Towfighi, J., Tavakkoli, M. (2016). Experimental investigation of bioethanol liquid phase dehydration using natural clinoptilolite. *Journal Advance Research* 7, 435-444. <https://doi.org/10.1016/j.jare.2016.02.009>.
- Karimi, S., Yarak, M.T., Karri, R.R. (2019) A comprehensive review of the adsorption mechanisms and factors influencing the adsorption process from the perspective of bioethanol dehydration. *Ren Sus En Rev* 107, 535 - 553. <https://doi.org/10.1016/j.rser.2019.03.025>
- Krochta, E.M. (1990). Emulsion films on food products to control mass transfer. En: *Food Emulsions and Foams*, (E.L. Gaden y E. Doi, eds.), Pp. 65-78. Plenum Press, Nueva York.
- Kuhns, R.J. and Shaw, G.H. (2018). *Navigating the Energy Maze: The Transition to a Sustainable Future*. Ed. Springer.
- Kupiec, K., Rakoczy, J., Komorowicz, T. and Larwa, B. (2014) Heat and mass transfer in adsorption-desorption cyclic process for ethanol dehydration. *Chem Eng J* 241, 485 - 494. <https://doi.org/10.1016/j.cej.2013.10.043>
- Morales-Martínez, J.L., Aguilar-Uscanga, M.G., Bolaños-Reynoso, E. and López-Zamora, L.. (2020). Optimization of chemical pretreatments using response surface methodology for 2nd generation ethanol production from coffee husk waste. *Bioenergy research*. <https://doi.org/10.1007/s12155-020-10197-6>.
- Partida-Sedas, G., Montes-García, N., Carvajal-Zarrabal, O., Lopez-Zamora, L., Gomez-Rodríguez, J. and Aguilar-Uscanga, M.G. (2016). Optimization of hydrolysis process to obtain fermentable sugars from sweet sorghum bagasse using a Box-Benken design. *Sugar Tech* 19, 317-325. <https://doi.org/10.1007/s12355-016-0461-y>
- Ribeiro, C.B., Martins, K.G., Gueri. M.V.D., Pavanello, G.P. and Schirmer, W.N. (2018). Effect of anhydrous ethanol/gasoline blends on performance and exhaust emissions of spark-ignited non-road engines. *Environ Science Pollution Research*. <https://doi.org/10.1007/s11356-018-2476-2>.
- Rumbo-Morales, J.Y., Lopez-Lopez, G., Alvarado, V.M., Valdez-Martinez, J.S., Sorcia-Vázquez, F.D.J. and Brizuela-Mendoza, J.A. (2018). Simulation and control of a pressure swing adsorption process to dehydrate ethanol. *Revista Mexicana de Ingeniería Química* 17, 1051-1081. <https://doi.org/10.24275/uam/izt/dcbi/revmexingquim/2018v17n3/Rumbo>
- Singh, A., Rangaiah, G.P. (2017). Review of technological advances in bioethanol recovery and dehydration. *Ind. Eng. Chem. Res.* 56, 5147 - 5163. <https://doi.org/10.1021/acs.iecr.7b00273>
- Smith, J.V. (1984). Definition of a zeolite. *Zeolites* 4, 309-310. [https://doi.org/10.1016/0144-2449\(84\)90003-4](https://doi.org/10.1016/0144-2449(84)90003-4)
- Teo, W.K., Ruthven, D.M. (1986). Adsorption of water from aqueous ethanol using 3-Å molecular sieves. *Industrial & Engineering Chemistry Process Design and Development* 25, 17 - 21. <https://doi.org/10.1021/i200032a003>
- Tihmillioglu, F., Ulku, S. (1996) Use of clinoptilolite in ethanol dehydration. *Separation Science and Technology* 31, 2855 - 2865. <https://doi.org/10.1080/01496399608000832>
- Wang, S., Peng, Y. (2010). Natural zeolites as effective adsorbents in water and wastewater treatment. *Chemical Engineering Journal* 156, 11-24. <https://doi.org/10.1016/j.cej.2011.11.110>
- Yamamoto, T., Han Kim, Y., Chul-Kim, B., Endo, A., Thongprachan, N., Ohmori, T. (2012). Adsorption characteristics of zeolites for dehydration of ethanol: evaluation of diffusivity of water in porous structure. *Journal of Chemistry Engineering* 181-182, 443 - 448. <https://doi.org/10.1016/j.cej.2011.11.110>